Macromolecules

Article

pubs.acs.org/Macromolecules

Photo-Cross-Linked Anion Exchange Membranes with Improved Water Management and Conductivity

S. Piril Ertem,[†] Tsung-Han Tsai,[†] Melissa M. Donahue,[†] Wenxu Zhang,[†] Himanshu Sarode,[‡] Ye Liu,[‡] Soenke Seifert,[§] Andrew M. Herring,[‡] and E. Bryan Coughlin*[,†]

[†]Department of Polymer Science and Engineering, University of Massachusetts Amherst, 120 Governors Drive, Amherst, Massachusetts 01003, United States

[‡]Department of Chemical and Biological Engineering, Colorado School of Mines, Golden, Colorado 80401, United States

[§]X-ray Science Division, Argonne National Laboratory, Argonne, Illinois 60439, United States

Supporting Information

ABSTRACT: Robust, cross-linked anion exchange membranes (AEMs) were prepared from solvent-processable polyisoprene-*ran*-poly(vinylbenzyltrimethylammonium chloride) (PI-*ran*-P[VBTMA][Cl]) ionomers via photoinitiated thiol−ene chemistry. Two series of membranes were prepared choosing two dithiol cross-linkers, 1,10-decanedithiol and 2,2′-(ethylenedioxy)diethanethiol, selected for their different hydrophobicities. A strong correlation was found between the choice of dithiol cross-linker, water uptake, morphology, and the ion conductivity of the membranes. Results were compared with previous findings of thermally cross-linked AEMs from analogous random copolymers. Comparably high chloride ion conductivities were obtained at low to moderate ion exchange capacities (IECs) with significantly low water uptake values. It was shown that by choosing a hydrophilic cross-linker ion cluster formation may be suppressed and ion conduction improved. This study highlights that it is possible to promote ion conductivities for low IEC membranes (<1 mmol/g) by forming well-connected, ion conducting network morphology. This observation paves the way for mechanically robust ion conducting membranes with enhanced conductivities and better water management.

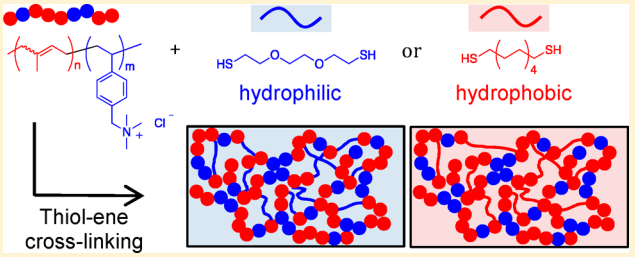

1. INTRODUCTION

Alkaline anion exchange membrane (AEM) fuel cells have been attracting increasing scientific interest over the past decade as a low-cost alternative to the proton exchange membrane (PEM) fuel cells.[1−4] Oxygen reduction and fuel oxidation reactions at the electrodes are kinetically more facile under alkaline conditions. Thus, non-noble metal catalysts can be used at the electrodes and operation costs can be greatly reduced. The electrokinetics also allows for a broader fuel choice, since low-carbon alcohols with high volumetric energy densities can be oxidized under high pH conditions.

There are several criteria to be met when designing AEMs: (i) high ion conductivities should be achieved at desired operation conditions (≥100 mS/cm), (ii) chemical and electrochemical stability under high alkaline environment, and (iii) sufficient mechanical robustness in a membrane electrode assembly. Ion conductivity is directly proportional to the diffusion coefficient and concentration of the conducting ion. Given the lower mobility of hydroxide ions compared to protons, it is challenging to reach high conductivities with AEMs as compared to PEMs. Increasing the ion exchange capacity (IEC), thus the fixed cation concentration in the membrane, is a way to enhance ion conductivity. However, mechanical integrity of the membranes is generally compromised at high IECs due to swelling of membranes caused by excessive water absorption.

An efficient way of preparing dimensionally stable robust AEMs is to introduce chemical or physical cross-links to the system. Different approaches were used to form cross-linked ionic networks: Semi-interpenetrated network approach was chosen to prepare membranes from quaternizable poly(ethylenimine) with poly(vinyl alcohol) matrix.[5] Quaternizable diamines were used to cross-link chloromethylated polysulfone or polystyrene backbones.[6−10] Similarly, already quaternized polymers or monomers with a cross-linkable functional group were used to form highly cross-linked anion conducting networks.[11−14] One of the most efficient methods was found to be ring-opening metathesis polymerization (ROMP). Clark et al. copolymerized tetraalkylammonium functionalized norbornene with a cross-linkable comonomer to obtain robust ion-conducting membranes.[14] Similarly, Robertson et al. prepared a cross-linked AEM through ROMP of cross-linkable ammonium cations with cyclooctene as comonomer.[13]

Received: August 11, 2015
Revised: November 16, 2015
Published: December 16, 2015

DOI: 10.1021/acs.macromol.5b01784
Macromolecules 2016, 49, 153−161

Optimized membranes had reasonable water uptake values, and chloride ion conductivities at high IECs.

A limiting factor for the above-mentioned systems is the control over membrane fabrication since polymerization and cross-linking occurs simultaneously during membrane casting. Solvent processability is a desired property for producing thin, durable ion exchange membranes. There are only a few examples for solvent processable ionic copolymers. A solvent processable tetraalkylammonium functionalized polyethylene was developed by Kostalik et al.[15] While the quaternized polymer was soluble in aqueous *n*-propanol, the solvent cast membrane remained water insoluble, likely due to the physical cross-links imparted by the semicrystalline nature of polyethylene. Gu et al. designed solvent processable polysulfones functionalized with triphenylphosphonium cations.[16,17] Solvent-cast membranes were thermally cross-linked through the Friedel−Crafts alkylation of the chloromethylated polymer backbone. We have previously reported the synthesis of water and methanol soluble isoprene containing ionomers.[18] Taking advantage of the remaining double bond functionality of isoprene units and their ability to cross-link under highly oxidative conditions we prepared thermally cross-linked membranes. In these systems, the extent of cross-linking was controlled by copolymer concentration, cross-linking temperature, and cross-linking time.

Thermal cross-linking generally requires high temperatures, and elongated reaction times. Side reactions also become more susceptible at high temperatures. To address this issue, Wang and Hickner prepared polystyrene based random, or block, copolymer ionomers with pendant alkene groups.[19] Olefin metathesis of these pendant alkenes provided a cross-linked network at room temperature. Similarly, Li et al. formed poly(phenylene oxide) based membranes with pendant alkene moieties cross-linked at room temperature using olefin metathesis.[20] While both of these cross-linking reactions were performed under ambient conditions, the obtained membranes were either not dimensionally stable enough, or the conductivity values were not as high as expected. Moreover, the synthesis of these materials require alkene-functionalized monomer synthesis, or post-polymerization modification, to incorporate cross-linkable moieties onto the polymer backbone.

Photo-cross-linking offers several advantages over thermal cross-linking: (i) ambient reaction temperatures greatly reduce possible side reactions, (ii) efficient cross-linking is achieved within seconds to minutes, (iii) the application area is readily adjustable, thus larger and thinner membranes can be prepared. Photoinduced radical mediated thiol−ene chemistry has been widely used to obtain cross-linked networks and to functionalize polymers.[21−23] The versatility of thiol−ene chemistry originates from its "click" type reaction characteristics: nearly quantitative yields can be achieved with considerably high reaction rates, requires minimal or no catalyst, can be applied in bulk or in solution, generates no side products, and there is a broad range of available thiols and alkenes. The insensitivity of thiol−ene reaction toward oxygen inhibition makes thiol−ene chemistry especially attractive for operations at ambient conditions.[21] Detailed reviews on thiol−ene chemistry and its various applications can be found in the literature.[22−24] To date there is only a few examples for photo-cross-linked AEMs prepared via thiol−ene chemistry. Stoicha et al. and Sollogoub et al. designed a polyelectrolyte using poly(epichlorohydrin-*co*-allylglacidyl ether) copolymer.[25−27] While the epichlorohydrin served as the quaternizable moiety, pendant double bonds of allylglycidyl ether moieties were used for cross-linking with a dithiol cross-linker. Recently, Tibbits et al. reported fabrication of AEMs with a single-step polymerization and cross-linking by photoinitiated thiol−ene chemistry.[28] In this work we present an approach to efficiently fabricate ion-conducting membranes from solvent-processable PI-*ran*-P[VBTMA][Cl] ionomers. The intrinsic double-bond functionality of the isoprene units provides the necessary alkene-functionality for thiol−ene chemistry. Breadth of available dithiols allowed choosing cross-linkers with desired physical properties. Robust ion-conducting membranes were obtained under mild reaction conditions and reduced cross-linking times.

2. EXPERIMENTAL SECTION

Materials. Isoprene (99%, Alfa Aesar) was distilled prior to use and stored under nitrogen. 4-vinylbenzyl chloride (VBCl) (90%, Acros Organics) was passed through a column of basic alumina. 3,7-Dioxa-4-aza-6-phosphanonanoic acid, 4,5-bis (1,1-dimethylethyl)-6-ethoxy-2,2-dimethyl-6-oxide (SG1) (BlockBuilder) was kindly provided by Arkema. 1,10-decanedithiol (Alpha Aesar), 2,2′-(ethylenedioxy)-ethanedithiol (Sigma-Aldrich), 1-dodacanethiol (Sigma-Aldrich), trimethylamine (50% aqueous solution, Acros Organics), and 2-Hydroxy-4′-(2-hydroxyethoxy)-2-methylpropiophenone (IRGACURE 2959, Sigma-Aldrich) were used without further purification.

General Polymerization Procedure for Polyisoprene-*ran*-poly(vinylbenzyl chloride) (PI-*ran*-PVBCl) Copolymers. The synthesis of PI-*ran*-PVBCl copolymers has been reported previously.[18] A typical polymerization procedure is as follows: isoprene (5.44 g, 80.0 mmol), vinylbenzyl chloride (8.15 g, 53.2 mmol) and SG1 (16 mg, 41.3 μmol) were transferred into a Teflon sealed Schlenk flask equipped with a magnetic stirrer. After three freeze−pump−thaw cycles the reaction flask was refilled with nitrogen gas. The copolymerization reaction was performed at 125 °C for 20 h. The reaction was quenched by cooling the flask in an ice bath. The viscous reaction mixture was diluted with dichloromethane and then precipitated into excess methanol to recover the copolymers as colorless solids.

General Procedure for Quaternization. Quaternization of PI-*ran*-PVBCl precursor were described in detail previously.[18] Approximately 1 g of precursor copolymer was weighed in a 20 mL syntillation vial. About 15 mL 50 wt % aqueous trimethylamine solution was added. The top of the vial was covered with Teflon tape and sealed tightly. The mixture was heated to 60 °C overnight. During the reaction the PI-*ran*-PVBCl copolymers dissolved in the aqueous reaction mixture. After the reaction water was removed under constant airflow, and subsequently under reduced pressure at 40 °C overnight to obtain the quaternized polymer polyisoprene-*ran*-poly(vinyl benzyl trimethylammonium chloride) (PI-*ran*-P[VBTMA][Cl]) as a pale yellow solid. Quaternized polymers were stored at −30 °C in the dark until used. The quaternized polymers are represented as PI-*ran*-P[VBTMA][Cl]-*x*, where *x* indicates the ion exchange capacity (IEC) of the polymer.

Instruments and Characterizations. ^{1}H NMR analysis was performed on a Bruker DPX-300 FT-NMR. Polymer Laboratories PL-GPC 50 integrated gel permeation chromatography (GPC) system was used to determine molecular weights and dispersity indices of the polymers calibrated against polystyrene standards in tetrahydrofuran at a flow rate of 1.0 mL/min using a refractive index detector. Infrared spectroscopy was performed on a PerkinElmer Spectrum 100 FT-IR spectrometer with universal attenuated total reflection (ATR) sampling accessory with a zinc selenide/diamond crystal. An average of four scans was collected with a resolution of 4 cm^{-1}. Ultraviolet (UV) irradiation was performed using an Oriel Flood Exposure System Model # 97435 (500 W mercury arc lamp, 365 nm) attached to a digital timer and a digital exposure controller.

The in-plane conductivity was analyzed using the membrane resistance measured with electrochemical impedance spectroscopy (EIS). The membrane was mounted in a four-probe test cell with

DOI: 10.1021/acs.macromol.5b01784
Macromolecules 2016, 49, 153−161

Table 1. Series of PI-*ran*-PVBCl Copolymers, Their Average Molecular Weight, Dispersity, Copolymer Compositions, and IEC of PI-*ran*-P[VBTMA][Cl]-*x* after Quaternization[a]

sample	PI-*ran*-PVBCl				PI-*ran*-P[VBTMA][Cl]
PI-*ran*-P[VBTMA][Cl]-*x*	M_n[b] (kg/mol)	$Đ$[b]	f_{VBCl}[c] NMR(%)	f_{VBCl}[d] feed(%)	IEC[e] (mmol/g)
PI-*ran*-P[VBTMA][Cl] 1.37	115	2.91	10.5	11.5	1.36
PI-*ran*-P[VBTMA][Cl] 1.68	55.1	3.10	15.0	15.1	1.68
PI-*ran*-P[VBTMA][Cl] 2.15	69.1	2.83	21.2	25.5	2.15
PI-*ran*-P[VBTMA][Cl] 2.29	68.3	3.57	23.2	26.2	2.29
PI-*ran*-P[VBTMA][Cl] 3.11	68.8	2.89	38.1	40.0	3.11

[a]*x* represents the IEC of the quaternized copolymers. [b]M_n and $Đ$ of PI-*ran*-PVBCl were measured by GPC with respect to PS standards. [c]Mole percent of VBCl as analyzed by ^{1}H NMR. [d]Mole percent of VBCl in the monomer feed. [e]IEC of copolymers prior to cross-linking was calculated based on the mole percent of VBCl as analyzed by ^{1}H NMR.

platinum electrodes with a constant separation distance. Impedance spectra were obtained over a frequency range of 1 Hz to 10 kHz. EIS data were collected using a Bio-Logic VMP3 potentiostat. During the measurements the samples were kept in a TestEquity H1000 oven to control temperature and relative humidity (RH). The temperature was varied from 50 to 90 °C by steps of 10 K at constant RH. Samples were allowed to equilibrate at each temperature set-point for 35 min before data collection. Collected data was analyzed using EC Laboratories software. eq 1 is used to convert resistance data to conductivity.

$$\sigma = \frac{L}{Rwt} \tag{1}$$

where R is the membrane polarization resistance, L is the distance between the electrodes, *w* and *t* are the width and the thickness of the sample, respectively.

Small angle X-ray scattering (SAXS) experiments were performed at the Advanced Photon Source at Argonne National Laboratory on beamline 12 ID-B. The X-ray beam has a wavelength of 1 Å and power of 12 keV. Scattering data was collected on a Pliatus 2 M SAXS detector with an acquisition time of 1 s. Integration of the 2D scattering pattern with respect to the scattering vector (q) provided the intensity (I) data. Temperature and humidity of the sample environment during SAXS measurements was controlled using a custom designed oven with four sample slots with Kapton windows, as described previously.[18,29,30] In a typical experiment, the oven was loaded with three membranes and one empty sample holder to collect a background spectrum of the environment for each experimental condition. Samples were soaked in water prior to loading. After removing the membranes from water, the superficial water was lightly dried with a Kimwipe. Samples were loaded into the oven at 60 °C at dry conditions. Loaded samples were allowed to equilibrate under dry gas flow for 20 min, and for 60 min at 95% RH, prior to X-ray measurement. The chamber temperature was kept constant as the RH was increased to 95% RH. Spectra were analyzed by subtracting the background wave of the corresponding experimental condition from the sample wave. Gaussian curve fitting was utilized to detect peak maxima of scattering curves.

Ion exchange capacity (IEC) is defined as milliequivalents of cations per gram of polymer, and was calculated from the ratio of VBCl to isoprene determined by ^{1}H NMR spectroscopy for each copolymer. IEC of membranes was experimentally determined by performing Mohr's titration. Approximately 80 mg of membrane was ion exchanged by stirring in 20 mL of 0.2 M $NaNO_3$(aq) solution. The solution was changed two times in total; first after 6 h, then after 17 h, to ensure complete ion exchange. The extraction solutions were collected and titrated against 0.105 M aqueous $AgNO_3$(aq) solution using K_2CrO_4 as indicator (2 mL, 0.25 M in water). The titrated IEC values were calculated from the dry mass of the membrane and the volume of $AgNO_3$(aq) consumed.

Hydration number (λ) defines the number of water molecules per cation. This value was calculated using the following equation:

$$\lambda = \frac{\left(\frac{m_{wet} - m_{dry}}{m_{dry}}\right) \times 1000}{MW_{water} \times IEC} \tag{2}$$

Dry mass (m_{dry}) of the membranes was determined after drying membranes under vacuum for 24 h. Membranes were soaked in water for 24 h prior to measuring the wet mass (m_{wet}). Before weighing the membranes for m_{wet}, the surface was gently wiped to remove excess water.

Membrane Fabrication and Photo-Cross-Linking Procedure. All membranes were prepared by drop-casting from a methanol solution following a similar procedure: PI-*ran*-P[VBTMA][Cl]-1.68 (200 mg) was weighed into an aluminum covered scintillation vial equipped with a magnetic stirrer. Photoinitiator solution (1.8 mL, 5.8 mg/mL in methanol) was then added. The contents of the vial were stirred until the polymer is dissolved. Three equivalents of dithiol cross-linker (120 μL 1,0-decanedithiol or 88 μL 2,2′-(ethylenedioxy)-ethanedithiol)) was added relative to the total amount of 1,2- and 3,4-isomers of isoprene units as estimated by ^{1}H NMR. The solution was thoroughly mixed in the dark for two more minutes. Membranes were then drop cast on a Teflon sheet and were covered with a Petri dish to allow slow evaporation of the solvent, and were allowed to dry at ambient conditions overnight in the dark. Cross-linking of the membranes was achieved by exposure to UV light for 10 min (365 nm, 100 mW/cm^2 at working distance).

3. RESULTS AND DISCUSSION

3.1. Ionomer Synthesis and Membrane Fabrication. A series of precursor copolymers poly(isoprene-*ran*-vinylbenzyl chloride) (PI-*ran*-PVBCl) were prepared through nitroxide mediated polymerization (NMP) of isoprene and 4-vinylbenzyl chloride (VBCl) (Table 1). The synthesis and characterization of similar copolymers were discussed previously.[18] The functional PI-*ran*-PVBCl precursors were quaternized through substitution of benzyl chloride groups with trimethylamine (TMA) to obtain benzyltrimethylammonium (BTMA) cations (Scheme 1). The copolymer ratio dictated the ion exchange capacities (IECs) of the quaternized PI-*ran*-P[VBTMA][Cl] ionomers. Theoretical IEC values of the ionomers were calculated using the copolymer ratios of the corresponding neutral precursors (Table 1). Nearly quantitative quaternization

Scheme 1. Quaternization of PI-*ran*-PVBCl To Form PI-*ran*-P[VBTMA][Cl] ionomers

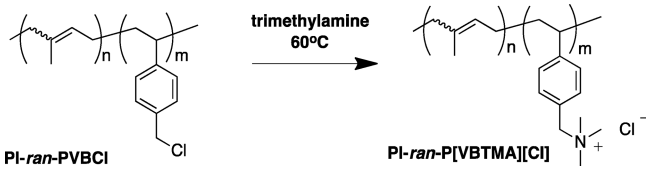

DOI: 10.1021/acs.macromol.5b01784
Macromolecules 2016, 49, 153−161

Table 2. Adjusted and Titrated IEC Values, % Water Uptake, Chloride Conductivity, and Average *d*-Spacing under Dry and Hydrated Environments[a]

PI-*ran*-P[VBTMA][Cl]-*x*	cross-linker	IEC_{adj}	IEC_{tit}	w.u.[b] (%)	λ	$\sigma_{60°C}$[c] (mS/cm)	$\sigma_{90°C}$[c] (mS/cm)	d_{dry}[d] (nm)	d_{wet}[e] (nm)
PI-*ran*-P[VBTMA][Cl] 1.37	DT	0.79	0.66	15.2	10.7	3.3	9.6	4.9	5.4
PI-*ran*-P[VBTMA][Cl] 1.68	DT	1.09	0.96	20.8	10.6	7.2	15.3	4.8	5.3
PI-*ran*-P[VBTMA][Cl] 2.15	DT	1.47	1.38	39.6	15.0	6.8	15.9	4.5	5.2
PI-*ran*-P[VBTMA][Cl] 2.29	DT	1.60	1.50	56.7	19.7	10.2	21.1	4.5	5.3
PI-*ran*-P[VBTMA][Cl] 3.11	DT	2.38	2.19	335	78.2	17.2	33.7	4.9	5.6
PI-*ran*-P[VBTMA][Cl] 1.37	EDDT	0.83	0.70	25.0	16.8	5.1	13.0	4.2	4.7
PI-*ran*-P[VBTMA][Cl] 1.68	EDDT	1.13	0.88	38.0	18.7	8.2	15.8	4.1	5.0
PI-*ran*-P[VBTMA][Cl] 2.15	EDDT	1.53	1.42	67.3	24.4	19.6	37.1	3.8	NA
PI-*ran*-P[VBTMA][Cl] 2.29	EDDT	1.66	1.48	115	38.5	7.1	11.1	3.8	5.2
PI-*ran*-P[VBTMA][Cl] 3.11	EDDT	2.45	2.28	437	99.0	n.d.	n.d.	3.4	NA

[a] *x* represents the IEC of the quaternized copolymers. [b] Water uptake. [c] Conductivity measurements are collected at 95% relative humidity. [d] Average distance between ionic clusters as determined from SAXS at 60 °C at dry conditions. [e] Average distance between ionic clusters as determined from SAXS at 60 °C at 95% relative humidity.

of the functional polymer precursors were confirmed by FT-IR analysis. Upon quaternization water and methanol soluble PI-*ran*-P[VBTMA][Cl] ionomers with moderate to high IECs were achieved.

It is known that isoprene tends to form three types of isomers during NMP: 1,4-addition, 1,2-addition, and 3,4-addition, where 1,4-addition is the dominant isomer.[31−33] Relative ratios of each isomer can be estimated from ^{1}H NMR by analyzing the vinyl proton signals. A representative ^{1}H NMR spectrum is shown in Figure S1. For the series of PI-*ran*-PVBCl copolymers listed in Table 1, the relative mole ratios of 1,4-, 1,2-, and 3,4- isomers were found to be around 90%, 4%, and 6%, respectively. It has been reported that the reactivity of alkenes toward thiol−ene reaction is inversely proportional to the extent of substitution.[34] While terminal alkenes with single substitution exhibit the highest reactivity, disubstitution reduces the reactivity significantly. It has also been noted that internal alkenes are less reactive than terminal alkenes due to steric effects. Thus, it can be expected that 1,2-isomer would be more reactive than 3,4-isomer, while 1,4-isomer would be the least reactive. A control experiment was designed to monitor the reactivity of the isoprene isomers toward thiol−ene reaction. The procedure and the findings can be found in the Supporting Information.

Considering that the sterically less hindered double bonds are more reactive, the amount of dithiol cross-linker was adjusted with respect to the total amount of pendant alkenes. The ene to dithiol ratio was optimized to 1:3 after detailed sol-fraction analyses (Supporting Information). Three membranes were prepared using the same PI-*ran*-P[VBTMA][Cl] precursor. Membranes were cross-linked using 1,10-decanedithiol (DT) with a pendant ene to dithiol ratio of 1:1, 1:2, and 1:3. Following photo-cross-linking the membranes were soaked into water. Since the ionomer precursor is soluble in water, any uncross-linked fraction would dissolve in water and would be detected by spectroscopic techniques. FT-IR spectra were collected for each sol-phase (Figure S3). When compared with the spectra of the neat DT and the uncross-linked PI-*ran*-P[VBTMA][Cl] precursor, at two folds excess of the stoichiometric amount of the pendant double bonds (1:1 ene:dithiol) vibrational peaks were observed that could be assigned to the uncross-linked residual polymer. As the dithiol ratio was increased to 1:2, the spectrum resembled more of a plain water spectrum. At 1:3 ene to dithiol ratio the spectrum did not show any residual polymer peaks within detection limits.

Two separate sets of membranes were prepared using two different dithiol cross-linkers with similar molecular weights: DT, as used previously, and 2,2′-(ethylenedioxy)diethanethiol (EDDT). The main difference between DT and EDDT was the slight hydrophilic character of EDDT imparted by the oxygen atoms, while DT has an intrinsic hydrophobic character due to its aliphatic hydrocarbon structure. The total mass of the network would increase with the addition of the cross-linkers. Therefore, the final IEC of the membranes would be lower than their corresponding precursor ionomers. The adjusted IECs were calculated for each of the membranes using the total mass of the network with the added dithiol cross-linker, and were confirmed experimentally by titration. The titration results were found to match with the adjusted IEC values, suggesting an efficient cross-linking (Table 2). The slightly lower IECs than the adjusted IEC values is likely due to incomplete ion exchange of chloride ions with nitrate ions during the ion exchange process. This would result in a lower chloride concentration of the analyte solution, thus an underestimated IEC value.

3.2. Characterization of the Photo-Cross-Linked Membranes.

3.2.1. Water Uptake Properties.

It is known that water plays a major role for ion-conducting membranes, as it was shown that the ion conductivity through polymeric media is highly dependent on the presence of water in the system.[18,35,36] However, water compromises the mechanical stability due to its plasticizing effect on ion-conducting membranes. Especially at high IECs, membranes usually absorb excessive amounts of water and become dimensionally unstable. Water uptake properties of both DT-cross-linked and EDDT-cross-linked membrane series were investigated. Both of the series showed low to moderate water uptake and λ values for IECs between 0.8 and 1.5 mmol/g and moderate to high water uptake at higher IECs. (Table 2, Figure 1) For IECs below 1.6 mmol/g, DT-cross-linked membranes had water uptake values around 15−57 wt %. Excessive water uptake at the highest IEC limit resulted a water uptake as high as 335 wt %.

EDDT-cross-linked membranes showed a similar trend: moderate to high water uptake for membranes with IECs below 1.66 mmol/g, and excessive water uptake for the highest IEC membrane. Overall, the water uptake values of the EDDT-cross-linked membranes were 1.5−2 times higher compared to the DT-cross-linked membranes at similar IECs. This

DOI: 10.1021/acs.macromol.5b01784
Macromolecules 2016, 49, 153−161

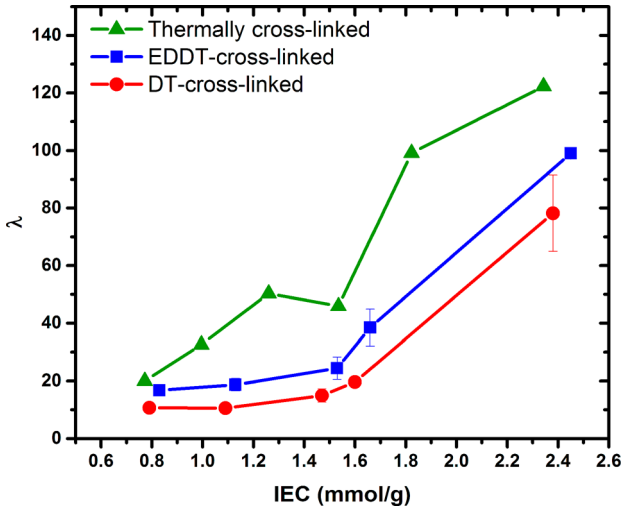

Figure 1. Hydration numbers (λ) of thermally cross-linked (triangles),[18] EDDT-cross-linked (squares), and DT-cross-linked (circles) membranes. Lines are drawn as a guide to the eye.

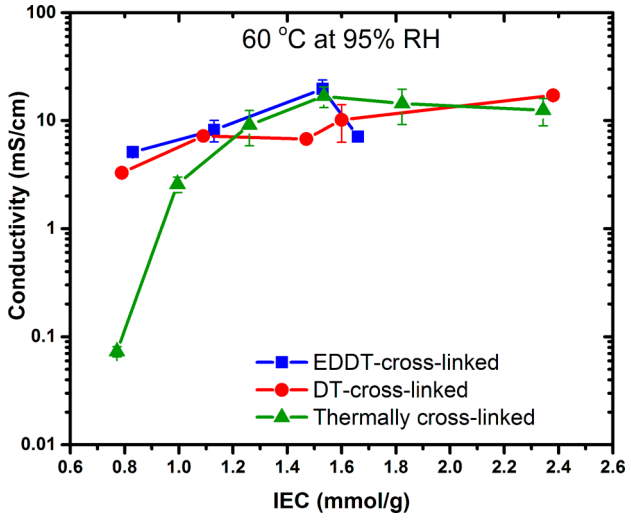

Figure 2. Ion conductivities of thermally cross-linked (triangles),[18] EDDT-cross-linked (squares), and DT-cross-linked (circles) membranes. Lines connect data points as a guide to the eye.

significant difference between the two series of membranes confirmed the increase in hydrophilic character of the membranes by incorporation of the hydrophilic EDDT cross-linker to the polymer network.

In both of the series, the highest IEC membranes experienced excessive water uptake. Precursors of the highest IEC membranes have a copolymer ratio of around 60 mol % isoprene and 40 mol % VBTMA. Since the pendant vinyl groups consist of only 8−10 mol % of the isoprene units, the cross-link density of these membranes presumably would not be sufficient to mitigate extreme swelling. At this IEC, the EDDT-cross-linked membrane swelled comparably more than the DT-cross-linked membrane. Also, the EDDT-cross-linked membrane was fragile and hard to manipulate. This is presumably due to slightly more hydrophilic character of EDDT-cross-linked membrane. This observation highlights the importance of a control over the water absorption to maintain the mechanical integrity of ion-conducting membranes.

3.2.2. Ion Conductivity Properties. Ion conductivity of the photo-cross-linked membranes was studied under temperature and humidity controlled environment. Accurate measurement of hydroxide ion conductivity at humidified conditions is a known challenge due to reactivity of hydroxide ions toward atmospheric carbon dioxide.[2,4] Also, stability of the cationic groups under alkaline conditions add another parameter to consider. While BTMA cations are stable enough for fundamental studies, ion conductivities of the photo-cross-linked membranes were collected with chloride as the conducting ion. The measurement results could then be interpreted without the influence of interfering conditions. Conductivity values at 60 and 90 °C are reported in Table 2 and are depicted in Figure 2.

DT-cross-linked membranes showed a monotonic increase of conductivity with increasing IEC. Highest conductivity was achieved from the highest IEC membrane. Chloride ion conductivities as high as 33.7 mS/cm were observed at 90 °C. While the conductivity values stayed within the same order of magnitude, nearly 5-fold increase was observed as IEC was increased from the lowest to the highest IEC (Table 2).

Conductivity of the EDDT-cross-linked membranes increased gradually until IEC 1.5 mmol/g, at which the highest conductivity was obtained. Beyond this IEC, conductivity decreased substantially. At IEC 1.66 mmol/g conductivity values were almost as low as the lowest IEC membrane. The highest IEC membrane was fragile when hydrated, such that the membrane was not easy to handle and mount to the instrument. Thus, data collection was not possible.

For the membranes with IECs around 1.5 mmol/g and below, EDDT-cross-linked membranes showed slightly higher conductivities than their DT-cross-linked counterparts. EDDT-cross-linked membranes reached their highest conductivities at IEC 1.53 mmol/g, while the DT-cross-linked membrane showed two to three times lower conductivity values at an equivalent IEC. This difference is likely due to the higher water uptake of EDDT-cross-linked membranes, as well as a more uniform distribution of water within the membrane. Because of slight hydrophilic character imparted by the EDDT cross-linker, absorbed water molecules are presumably drawn into the cross-linked network. Thus, the water molecules would not be localized only around BTMA moieties, and would likely infuse into the cross-linked network surrounding the ionic moieties. Therefore, in EDDT-cross-linked membranes ions would likely be transferred between BTMA moieties through the delocalized aqueous medium.

DT-cross-linked membranes showed as high conductivities as the EDDT-cross-linked membranes only at their highest IEC limit. While this could be explained by the high water content, the amount of water molecules to render this conductivity is much higher than it is for the EDDT-cross-linked membrane at IEC 1.53 mmol/g. DT-cross-linked membrane at IEC 1.60 mmol/g absorbed similar amount of water (λ = 19.7) to the highest conducting EDDT-cross-linked membrane. However, the conductivity values were still lower than the EDDT-cross-linked membrane, despite the slightly higher IEC.

It was found that the diffusion coefficient of the conducting ion approximates its dilute solution diffusivity limit, when ion-conducting membranes are sufficiently hydrated.[11,37] It is also known that conductivity is a function of diffusion coefficient, and these values are directly proportional.[35] Therefore, once the dilute solution conditions are reached, it would likely not be possible to increase the conductivity further by increasing the IEC.[18] The conductivity of the DT-cross-linked membranes at

DOI: 10.1021/acs.macromol.5b01784
Macromolecules 2016, 49, 153−161

the highest IEC were presumably collected close to dilute solution conditions, given the large water content in the membrane, and thus the highest conductivity possible was achieved at this IEC. In general, these conductivity values were relatively high. By comparison, Robertson et al. reported 24.6 mS/cm chloride conductivity for a membrane at IEC 2.3 mmol/g.[13] This value was collected while the membrane was immersed in water at 50 °C.

While these observations emphasize the role of water for ion conductivity, it is also evident that the distribution of water within the membrane plays a critical role for efficient ion transport through a polymeric medium. However, excessive water absorption needs to be avoided to maintain the mechanical stability of the membrane.

3.2.3. Morphology of the Photo-Cross-Linked Membranes. Morphologies of the photo-cross-linked membranes were investigated with SAXS under environmentally controlled conditions. Figure 3 and Figure 4 show the SAXS patterns of

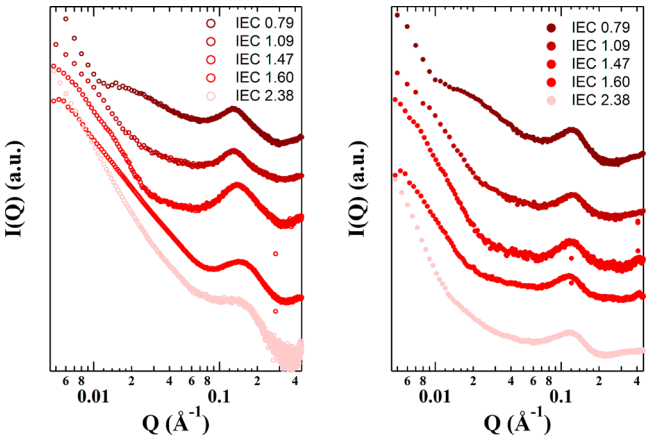

Figure 3. SAXS data for DT-cross-linked membranes at dry (left) and 95% RH (right) environment. Spectra are offset along the *y*-axis for clarity.

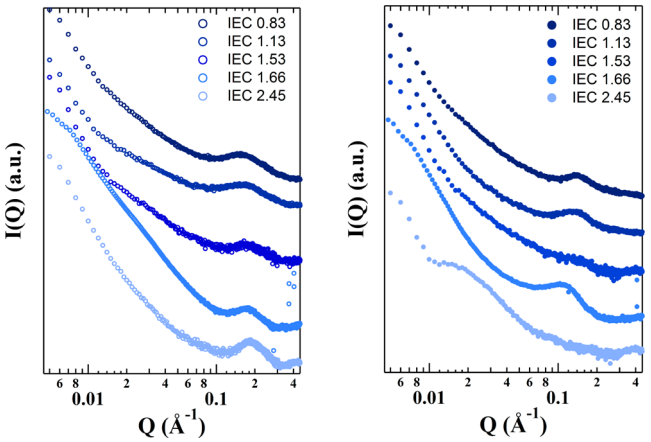

Figure 4. SAXS data for EDDT-cross-linked membranes at dry (left) and 95% RH (right) environment. Spectra are offset along the *y*-axis for clarity.

the DT-cross-linked and EDDT-cross-linked membranes, respectively, at 60 °C under dry and 95% relative humidity conditions. Membranes of both series showed a scattering peak around 0.1−0.2 Å^{-1} reminiscent of the ionomer peak of hydrated Nafion.[38−40] The electron density contrast is rendered by the chloride ions. Therefore, these scattering peaks were attributed to microphase separation of BTMA moieties, presumably to form ion clusters.

When dry, DT-cross-linked membranes showed an average *d*-spacing between ion clusters in the range of 4.5−4.9 nm. A monotonic decrease of *d*-spacing was observed with increasing IEC. This decrease indicates formation of ion clusters that are closer to each other with decreasing volume of the nonionic network surrounding the BTMA moieties. The highest IEC membrane deviates from this trend and shows a *d*-spacing similar to the *d*-spacing of the lowest IEC membrane. This deviation suggests a stronger microphase separation between the ionic and the nonionic domains, presumably due to high mole fraction of the BTMA groups on the PI-*ran*-P[VBTMA]-[Cl] precursor, and thus strong incompatibility with the DT cross-linked network.

When hydrated, a slight shift of the scattering peaks toward higher scattering angles was observed, indicative of the swelling of the membranes as the hygroscopic ion clusters absorb water. The change in average *d*-spacing from dry to hydrated state becomes more pronounced as the IEC is increased. This is likely due to higher water uptake of the membrane with increasing IEC, as well as the reduced volume fraction of the cross-linked network, thus less support to swelling ionic clusters. The peak intensities and peak width at half-maximum stay rather similar upon hydration. This indicates that the ion clusters do not undergo a significant rearrangement to form well-defined clusters. Swelling of the ion clusters are presumably restricted by the surrounding cross-linked hydrophobic matrix. Therefore, swelling of the clusters, and thus the membranes, is limited.

Similarly, EDDT-cross-linked membranes show a decreasing trend of *d*-spacing with increasing IEC, when dry. In general, intercluster spacing of EDDT-cross-linked membranes was found to be smaller than the DT-cross-linked membranes. At 95% relative humidity, the scattering peaks shifted toward lower scattering angles. This shift was more pronounced compared to the DT-cross-linked membranes, suggesting that EDDT-cross-linked membranes swelled more, presumably due to their higher water uptake. The scattering peak intensity decreased remarkably after hydration. Scattering peaks of the membranes with IECs 1.53 mmol/g and 2.45 mmol/g disappeared almost completely upon hydration. The latter showed a shoulder at lower scattering angles suggesting phase separation of larger length scales (30−40 nm). Absence of the scattering peak around 0.12 Å indicates a more uniform distribution of the chloride ions within the hydrated membranes. As discussed earlier, the hydrophilic EDDT cross-linker likely induces absorption of the water molecules by the cross-linked network surrounding the ion clusters. The dissociated chloride ions can presumably diffuse into the cross-linked network. Thus, chloride ions are not localized to the ion clusters. The delocalization of the chloride ions is also likely the reason for relatively weaker scattering peaks of the hydrophilic membranes in their hydrated state.

3.3. Correlation of the Morphology with the Ion Conductivity. Many studies have shown the effect of an interconnected microphase-separated morphology on ion conductivity.[41−44] Findings indicated that a connected ionic network is an important factor to promote ion conductivity. Studies have shown that block copolymers generally exhibit higher conductivities than the random copolymer analogues due to their strong microphase-separated morphology.[45−47]

DOI: 10.1021/acs.macromol.5b01784
Macromolecules 2016, 49, 153−161

However, the connectivity of the ionic domains is influenced by multiple factors such as the microphase-separated morphology,[48] grain size and structure,[49] and the anisotropic alignment of the ionic domains in the direction of conduction.[46,49,50] The microphase-separated morphology can be controlled by adjusting the volume fractions of each block, however a connected network morphology (gyroid) is difficult to achieve. Moreover, ionic block copolymers may show unusual phase separation behavior due to large chemical mismatch between the ionic and the nonionic blocks.[51,52] Grain size and the isotropic alignment of the ionic domains depend on many other factors such as the choice of film casting solvent, the membrane preparation technique, and the thermal history of the polymer membrane. Therefore, desired connected morphologies, and thus ion conductivities, may not be readily obtained.

Our findings indicate that a connected ion pathway might be obtained using random copolymers. The SAXS results of each membrane were correlated with the ion conductivity obtained under similar conditions. Hydrated membranes exhibited an average distance between ionic clusters around 4.7−5.6 nm. These distances match with the previously reported *d*-spacing range for various other ion-conducting membranes.[53] These values also correlate with our findings with thermally cross-linked analogous membranes, where we proposed a critical *d*-spacing below witch a percolated ionic network may have formed. This correlation is discussed in detail in the following section.

The highest conductivity was measured at IEC 1.54 mmol/g for the EDDT-cross-linked membrane series. This high conductivity was attributed to a more uniform distribution of water molecules within the cross-linked network. Absence of the scattering peak at this IEC for the humidified membrane indicates a uniform distribution of the chloride ions with inclusion of water to the system, supporting a uniform distribution of water within the membrane. DT-cross-linked membranes exhibited almost 3 times lower conductivity at a similar IEC (1.47 mmol/g). At this IEC a scattering peak was observed corresponding to an average *d*-spacing around 5.2 nm.

The effect of a uniform distribution of ions can also be observed by comparing the conductivities of the two membrane systems at other IEC values. At IEC around 1.1 mmol/g EDDT-cross-linked membranes have slightly higher ion conductivity then the DT-cross-linked membranes, while both membranes have a *d*-spacing around 5 nm. Increasing IEC from 1.09 to 1.47 mmol/g does not significantly improve chloride conductivity for the DT-cross-linked membrane, and the *d*-spacing between ionic clusters remain almost constant. For similar IEC transition with the EDDT-cross-linked membranes the ion conductivity increases nearly 2.5 fold while the ion cluster peak vanishes. It is important to point out that the change in λ value for this IEC transition is around 5 water molecules for both of the membrane systems. These observations strongly suggest that a more uniform distribution of water molecules within the membrane might facilitate ion transport between clusters.

Beers and Balsara demonstrated that ion clusters may obstruct ion transport by designing a block copolymer membrane with a cluster-free ionic domain.[53] Cluster-free ionic domains were achieved at a narrow lamellar *d*-spacing ($\leq$12 nm). However, it is nontrivial to achieve robust block copolymer membranes with such small average *d*-spacing, since high molecular weights are necessary to provide molecular entanglements for desired mechanical properties. Moreover, for block copolymers, the extent of phase separation depends on average block molecular weight and other factors, as listed above. Our observations demonstrate that the effect of ion clustering on ion conductivity could be suppressed by tuning the hydrophilicity/hydrophobicity of the network surrounding the ion clusters. By this approach, highly ion-conducting membranes can be obtained without sacrificing mechanical robustness. Moreover, the disordered morphology of the random copolymers would allow easier membrane processing.

3.4. Comparison of Photo-Cross-Linked Membranes with Their Thermally Cross-Linked Counterparts. In our previous report we discussed preparation and characterization of thermally cross-linked membranes of PI-*ran*-P[VBTMA][Cl] ionomers.[18] Photo-cross-linked membranes were prepared using similar ionomers with higher IECs. The addition of a cross-linker increased the overall mass of the network, thus resulting in a reduced IEC. The final IECs of the photo-cross-linked networks were comparable to the IECs of the thermally cross-linked counterparts.

Both photo-cross-linked membrane series absorbed comparably less water than their thermally cross-linked counterparts at a comparable IEC (Figure 2). While the EDDT-cross-linked membranes absorbed more water than the DT-cross-linked membranes, the overall water uptake values of the photo-cross-linked membranes were still lower than the thermally cross-linked membranes. Generally, photo-cross-linked membranes swelled comparably less than the analogous thermally cross-linked membranes.[54] These observations suggest that photo-cross-linking allows for better control over cross-link density.

It is important to point out that despite the lower water uptake value, the EDDT-cross-linked membrane at the highest IEC was more fragile compared to the thermally cross-linked membranes at their highest IEC. The thermally cross-linked membrane was formed from a PI-*ran*-P[VBTMA][Cl] precursor with 24 mol % isoprene, while its photo-cross-linked equivalent consists of 38 mol % isoprene. Thus, photo-cross-linked membrane contained less available cross-linking sites. This compositional difference likely is a reason for the fragile nature of the hydrated EDDT-cross-linked membrane at high IEC limit. DT-cross-linked membranes with IEC 2.38 mmol/g, on the other hand, were not as fragile. The softness of the EDDT-cross-linked membrane is presumably due to plasticizing effect of water that is absorbed by the EDDT units of the cross-linked network.

When ion conductivities were compared, the most remarkable difference of the photo-cross-linked membranes from their thermally cross-linked counterparts is their equivalent or higher conductivity values despite their comparably lower water uptake (Figure 2). In particular, at the lowest IEC limit, both EDDT- and DT-cross-linked membranes show almost 2 orders of magnitude higher conductivities than the thermally cross-linked membrane with IEC 0.77 mmol/g. At this IEC thermally cross-linked membranes absorbed around 30 wt % water (λ = 20). While the EDDT-cross-linked membranes absorbed similar amount of water at a similar IEC, DT-cross-linked membranes still absorbed half of the amount of what thermally cross-linked membranes absorb. This observation strongly suggests that efficient ion conductivity cannot be solely explained by the extent of water uptake or ion concentration.

The scattering profiles of the photo-cross-linked membranes exhibit clear differences to their thermally cross-linked counterparts, providing an understanding of the difference

DOI: 10.1021/acs.macromol.5b01784
Macromolecules 2016, 49, 153−161

between the conductivities of thermally and photo-cross-linked membranes at their lowest IEC limit. In our discussion on the thermally cross-linked PI-*ran*-P[VBTMA][Cl] membranes we found a strong correlation between morphology and ion conductivity.[18] When the *d*-spacing between ionic clusters was below a critical distance (5.0−5.6 nm) the ion conductivity improved significantly. This was attributed to formation of a percolated network of ionic clusters. The largest average *d*-spacing obtained from hydrated photo-cross-linked membranes was 5.6 nm (Table 2). At their lowest IEC hydrated DT- and EDDT-cross-linked membranes formed clusters with an average *d*-spacing of 5.4 and 4.7 nm, respectively. Hydrated thermally cross-linked membranes with IEC 0.77 mmol/g had an average *d*-spacing around 6 nm. This observation matches well with our previous findings, and suggests an interconnected ionic network formation below a critical *d*-spacing. It also indicates that membranes with low IEC, and therefore low water content, may exhibit high ion conductivities, if the correct morphology is achieved. This could lead the way for preparation of robust and high ion-conducting membranes with better water management.

Other important findings of the SAXS results are the differences of change in peak intensity and the peak position with the change in relative humidity. Scattering peaks of thermally cross-linked membranes became sharper and more intense with inclusion of water, indicating formation of better-defined ion clusters. Photo-cross-linked membranes, on the other hand, did not show a significant change in scattering peak intensity. In the case of EDDT-cross-linked membranes, the peak intensities decreased, such that some membranes did not scatter when hydrated due to uniform ion distribution. Peak shifts of the photo-cross-linked membranes were relatively less pronounced compared to the thermally cross-linked membranes. This indicates a well-cross-linked network formation for photo-cross-linked membranes with more confined ionic clusters.

Mechanical properties of thermally and photo-cross-linked membranes under temperature and humidity controlled environment was reported recently.[54] Using similar precursor ionomers a DT-cross-linked membrane and two thermally cross-linked membranes were prepared applying different cross-linking times (3 and 24 h). Here the reader should be informed that the overall IEC of the photo-cross-linked membrane was about 1.5 times lower than the thermally cross-linked membranes due to the added cross-linker. For the thermally cross-linked membranes the mechanical properties were found to be strongly dependent on the cross-linking time, as well as the changes in the ambient conditions. In general, photo-cross-linked membranes showed more consistent dimensional and mechanical stability, when hydrated. The findings of this study indicated that photoinduced thiol−ene cross-linking approach is a reliable technique to prepare cross-linked ion-conducting networks in significantly shorter times.

4. Conclusions. Ion-conducting membranes were prepared using isoprene containing solvent processable ionomers. Robust membranes were obtained by cross-linking the membranes using thiol−ene chemistry taking advantage of the remaining unsaturation on the polymer backbone. Two different dithiol cross-linkers were used to prepare two separate series of cross-linked membranes with a range of IEC values. The difference between the chemical structures of the dithiol cross-linkers affected the water uptake profile of the series. Membranes with more hydrophilic cross-linker absorbed comparably more water. Photo-cross-linked membranes showed ion conductivities within the same order of magnitude, where the EDDT-cross-linked membranes exhibited slightly higher conductivities. This difference was attributed to higher water content within the EDDT-cross-linked network. Also, a strong correlation was found between the ion conductivity and the morphology of the membranes. Photo-cross-linked membranes formed ion clusters with an average *d*-spacing around 5.6 nm and smaller. Some of the membranes lacked the ion cluster peak when hydrated. The highest ion conductivity value was obtained from the membrane without the ion cluster peak. This observation suggested that a uniform distribution of conducting ions might promote ion conduction through polymeric media. Finally, and most importantly, it was shown that high ion conductivities can be obtained from low IEC membranes with relatively low water contents. This observation highlights the necessity to achieve a percolated network for efficient ion conduction through polymeric media. With a better understanding of the control over the desired morphology, highly conducting robust membranes with improved water management can be obtained.

■ ASSOCIATED CONTENT

Supporting Information

The Supporting Information is available free of charge on the ACS Publications website at DOI: 10.1021/acs.macromol.5b01784.

^{1}H NMR of PI-*ran*-PVBCl copolymers before quaternization, experimental procedure for the control experiment for thiol−ene reaction efficiency with polyisoprene units, ^{1}H NMR of PI-*ran*-PVBCl precursors before and after thiol−ene reaction, experimental procedure for sol-fraction analysis, and FT-IR of sol-fraction of the photo-cross-linked PI-*ran*-P[VBTMA][Cl] copolymer with increasing ene to dithiol ratio (PDF)

■ AUTHOR INFORMATION

Corresponding Author

*(E.B.C.) E-mail: Coughlin@mail.pse.umass.edu.

Notes

The authors declare no competing financial interest.

■ ACKNOWLEDGMENTS

This material is based upon work supported by, or in part by, the U.S. Army Research Laboratory and the U.S. Army Research Office under MURI Contract/Grant Number W911NF-10-1-0520. This research used resources of the Advanced Photon Source, a U.S. Department of Energy (DOE) Office of Science User Facility operated for the DOE Office of Science by Argonne National Laboratory under Contract No. DE-AC02-06CH11357.

■ REFERENCES

(1) Merle, G.; Wessling, M.; Nijmeijer, K. *J. Membr. Sci.* **2011**, *377*, 1−35.

(2) Hickner, M. A.; Herring, A. M.; Coughlin, E. B. *J. Polym. Sci., Part B: Polym. Phys.* **2013**, *51*, 1727−1735.

(3) Varcoe, J. R.; Slade, R. C. T. *Fuel Cells* **2005**, *5*, 187−200.

(4) Varcoe, J. R.; Atanassov, P.; Dekel, D. R.; Herring, A. M.; Hickner, M. A.; Kohl, P. A.; Kucernak, A. R.; Mustain, W. E.; Nijmeijer, K.; Scott, K.; Xu, T.; Zhuang, L. *Energy Environ. Sci.* **2014**, *7*, 3135−3191.

DOI: 10.1021/acs.macromol.5b01784
Macromolecules 2016, 49, 153−161

(5) Yu Xu, P.; Yi Guo, T.; Hui Zhao, C.; Broadwell, I.; Gen Zhang, Q.; Liu, Q. L. *J. Appl. Polym. Sci.* **2013**, *128*, 3853−3860.
(6) Hao, J. H.; Chen, C.; Li, L.; Yu, L.; Jiang, W. *Desalination* **2000**, *129*, 15−22.
(7) Komkova, E.; Stamatialis, D.; Strathmann, H.; Wessling, M. *J. Membr. Sci.* **2004**, *244*, 25−34.
(8) Varcoe, J. R.; Slade, R. C. T.; Lam How Yee, E. *Chem. Commun. (Cambridge, U. K.)* **2006**, 1428−1429.
(9) Park, J.-S.; Park, S.-H.; Yim, S.-D.; Yoon, Y.-G.; Lee, W.-Y.; Kim, C.-S. *J. Power Sources* **2008**, *178*, 620−626.
(10) Pan, J.; Chen, C.; Zhuang, L.; Lu, J. *Acc. Chem. Res.* **2012**, *45*, 473−481.
(11) Zha, Y.; Disabb-Miller, M. L.; Johnson, Z. D.; Hickner, M. A.; Tew, G. N. *J. Am. Chem. Soc.* **2012**, *134*, 4493−4496.
(12) Price, S. C.; Ren, X.; Jackson, A. C.; Ye, Y.; Elabd, Y. A.; Beyer, F. L. *Macromolecules* **2013**, *46*, 7332−7340.
(13) Robertson, N. J.; Kostalik, H. A., IV; Clark, T. J.; Mutolo, P. F.; Abrun a, H. D.; Coates, G. W. *J. Am. Chem. Soc.* **2010**, *132*, 3400−3404.
(14) Clark, T. J.; Robertson, N. J.; Kostalik, H. A., IV; Lobkovsky, E. B.; Mutolo, P. F.; Abrun a, H. D.; Coates, G. W. *J. Am. Chem. Soc.* **2009**, *131*, 12888−12889.
(15) Kostalik, H. A., IV; Clark, T. J.; Robertson, N. J.; Mutolo, P. F.; Longo, J. M.; Abruña, H. D.; Coates, G. W. *Macromolecules* **2010**, *43*, 7147−7150.
(16) Gu, S.; Cai, R.; Yan, Y. *Chem. Commun. (Cambridge, U. K.)* **2011**, *47*, 2856−2858.
(17) Gu, S.; Cai, R.; Luo, T.; Chen, Z.; Sun, M.; Liu, Y.; He, G.; Yan, Y. *Angew. Chem., Int. Ed.* **2009**, *48*, 6499−6502.
(18) Tsai, T.; Ertem, S. P.; Maes, A. M.; Seifert, S.; Herring, A. M.; Coughlin, E. B. *Macromolecules* **2015**, *48*, 655−662.
(19) Wang, L.; Hickner, M. A. *Polym. Chem.* **2014**, *5*, 2928.
(20) Li, N.; Wang, L.; Hickner, M. A. *Chem. Commun. (Cambridge, U. K.)* **2014**, *50*, 4092−4095.
(21) Hoyle, C. E.; Lee, T. Y.; Roper, T. M. *J. Polym. Sci., Part A: Polym. Chem.* **2004**, *42*, 5301−5338.
(22) Hoyle, C. E.; Bowman, C. N. *Angew. Chem., Int. Ed.* **2010**, *49*, 1540−1573.
(23) Kade, M. J.; Burke, D. J.; Hawker, C. J. *J. Polym. Sci., Part A: Polym. Chem.* **2010**, *48*, 743−750.
(24) Lowe, A. B. *Polym. Chem.* **2014**, *5*, 4820.
(25) Stoica, D.; Ogier, L.; Akrour, L.; Alloin, F.; Fauvarque, J.-F. *Electrochim. Acta* **2007**, *53*, 1596−1603.
(26) Stoica, D.; Alloin, F.; Marais, S.; Langevin, D.; Chappey, C.; Judeinstein, P. *J. Phys. Chem. B* **2008**, *112*, 12338−12346.
(27) Sollogoub, C.; Guinault, A.; Bonnebat, C.; Bennjima, M.; Akrour, L.; Fauvarque, J. F.; Ogier, L. *J. Membr. Sci.* **2009**, *335*, 37−42.
(28) Tibbits, A. C.; Mumper, L. E.; Kloxin, C. J.; Yan, Y. S. *J. Electrochem. Soc.* **2015**, *162*, F1206−F1211.
(29) Schlichting, G. J.; Horan, J. L.; Jessop, J. D.; Nelson, S. E.; Seifert, S.; Yang, Y.; Herring, A. M. *Macromolecules* **2012**, *45*, 3874−3882.
(30) Liu, Y.; Horan, J. L.; Schlichting, G. J.; Caire, B. R.; Liberatore, M. W.; Hamrock, S. J.; Haugen, G. M.; Yandrasits, M. A.; Seifert, S.; Herring, A. M. *Macromolecules* **2012**, *45*, 7495−7503.
(31) Jitchum, V.; Perrier, S. *Macromolecules* **2007**, *40*, 1408−1412.
(32) Harrisson, S.; Couvreur, P.; Nicolas, J. *Macromolecules* **2011**, *44*, 9230−9238.
(33) Benoit, D.; Harth, E.; Fox, P.; Waymouth, R. M.; Hawker, C. J. *Macromolecules* **2000**, *33*, 363−370.
(34) Roper, T. M.; Guymon, C. A.; Jonsson, E. S.; Hoyle, C. E. *J. Polym. Sci., Part A: Polym. Chem.* **2004**, *42*, 6283−6298.
(35) Hickner, M. A. *J. Polym. Sci., Part B: Polym. Phys.* **2012**, *50*, 9−20.
(36) Peckham, T. J.; Holdcroft, S. *Adv. Mater.* **2010**, *22*, 4667−4690.
(37) Disabb-Miller, M. L.; Johnson, Z. D.; Hickner, M. A. *Macromolecules* **2013**, *46*, 949−956.
(38) Schmidt-Rohr, K.; Chen, Q. *Nat. Mater.* **2008**, *7*, 75−83.
(39) Mauritz, K. A.; Moore, R. B. *Chem. Rev.* **2004**, *104*, 4535−4585.
(40) Kreuer, K. D.; Portale, G. *Adv. Funct. Mater.* **2013**, *23*, 5390−5397.
(41) Li, N.; Guiver, M. D. *Macromolecules* **2014**, *47*, 2175−2198.
(42) Pan, J.; Chen, C.; Li, Y.; Wang, L.; Tan, L.; Li, G.; Tang, X.; Xiao, L.; Lu, J.; Zhuang, L. *Energy Environ. Sci.* **2014**, *7*, 354.
(43) Choi, J. H.; Ye, Y.; Elabd, Y. a.; Winey, K. I. *Macromolecules* **2013**, *46*, 5290−5300.
(44) Tsai, T.-H.; Maes, A. M.; Vandiver, M. a.; Versek, C.; Seifert, S.; Tuominen, M.; Liberatore, M. W.; Herring, A. M.; Coughlin, E. B. *J. Polym. Sci., Part B: Polym. Phys.* **2013**, *51*, 1751−1760.
(45) Tanaka, M.; Fukasawa, K.; Nishino, E.; Yamaguchi, S.; Yamada, K.; Tanaka, H.; Bae, B.; Miyatake, K.; Watanabe, M. *J. Am. Chem. Soc.* **2011**, *133*, 10646−10654.
(46) Elabd, Y. A.; Napadensky, E.; Walker, C. W.; Winey, K. I. *Macromolecules* **2006**, *39*, 399−407.
(47) Ye, Y.; Sharick, S.; Davis, E. M.; Winey, K. I.; Elabd, Y. A. *ACS Macro Lett.* **2013**, *2*, 575−580.
(48) Weber, R. L.; Ye, Y.; Schmitt, A. L.; Banik, S. M.; Elabd, Y. A.; Mahanthappa, M. K. *Macromolecules* **2011**, *44*, 5727−5735.
(49) Chintapalli, M.; Chen, X. C.; Thelen, J. L.; Teran, A. a; Wang, X.; Garetz, B. a; Balsara, N. P. *Macromolecules* **2014**, *47*, 5424−5431.
(50) Park, M. J.; Balsara, N. P. *Macromolecules* **2010**, *43*, 292−298.
(51) Wang, X.; Goswami, M.; Kumar, R.; Sumpter, B. G.; Mays, J. *Soft Matter* **2012**, *8*, 3036.
(52) Sudre, G.; Inceoglu, S.; Cotanda, P.; Balsara, N. P. *Macromolecules* **2013**, *46*, 1519−1527.
(53) Beers, K. M.; Balsara, N. P. *ACS Macro Lett.* **2012**, *1*, 1155−1160.
(54) Vandiver, M. a.; Caire, B. R.; Ertem, S. P.; Tsai, T.; Coughlin, E. B.; Herring, A. M.; Liberatore, M. W. *J. Electrochem. Soc.* **2015**, *162*, H206−H212.

DOI: 10.1021/acs.macromol.5b01784
Macromolecules 2016, 49, 153−161